Neural Networks-Based Tool for Diagnosis of Paranasal Sinuses Conditions

Abdel–Razzak Natsheh, Prasad VS Ponnapalli, Nader Anani, Dalil Benchebra and Atef El-kholy*
Manchester Metropolitan University, Manchester M1 5GD, UK
*Trafford General Hospital, Manchester M41 5SL, UK
a.natsheh@mmu.ac.uk n.anani@mmu.ac.uk, p.ponnapalli@mmu.ac.uk, atefelkholy@hotmail.com

Abstract—**This paper describes the development of a neural networks-based software system for the analysis and diagnosis of sinus conditions. Traditional image processing techniques and artificial neural networks tools and algorithms such as the self-organizing maps (SOM) were invoked in the development of the diagnosis system. The data were in the form of anonymous CT-images of sinuses obtained from a local hospital. A major problem faced the development of the system was caused by the fragmented or incomplete boundaries between different objects in the CT-images. A new algorithm was developed and successfully applied to complete such boundaries. The system was thoroughly tested with real images and the results indicate a potential for the system to be integrated within a CT-scanning system to automate the process of diagnosis.**

I. Introduction

Due to the similarity and nature of the sinuses diseases and the complexity of their medical images, e.g. CT-scans, which are used for the assessment of their conditions, their initial diagnosis can be a fairly complex and demanding process. It involves the use of multiple sources of information (e.g. laboratory and visual tests, CT-scans). Further, the diagnosis process requires normally the expertise of a radiologist in addition to the ENT (Ear throat and Nose) consultant.

During the diagnosis an ENT doctor has to use multiple threads of reasoning employing qualitative and quantitative measures to arrive at a diagnosis. Such decisions are harder to make when the related etiology is hard to discern or when multiple diseases are suffered [1]. Discussions with ENT consultants and radiologists highlighted the need for an automated computer-based analysis and diagnosis tool that can be used, not only as an aid to experts, but also for use in the training of doctors and medical students.

Such a tool, the Sinus Diagnostic System, henceforth referred to as the (SDS) has been developed using techniques based on classical image processing algorithms and procedures in conjunction with Artificial Neural Networks (ANNs) tools. Previous work reported the potential benefits of using ANNs in enhancing early diagnosis [2].

The proposed SDS consists of two main stages: the first stage involves identification of the Region of Interest (ROI) that represents the four sinus areas: maxillary, ethmoid, sphenoid and frontal depicted in Figure 1. The second stage consists of analysis of the sinus areas using a technique based on a class of ANNs known as the Self-Organizing Maps. One of the problems faced the development of the sinus diagnosis system was the extraction of the ROI or the sinus areas from CT-images, Figure 2. A number of algorithms have been invoked and tested for this purpose; edge detection methods [3,4], active contours [5,6,7], and watershed transformation [8,9]. However, the majority of those methods require prior information about the expected features of the image and hence some sort of user interaction is required. This defies the purpose of the proposed system which aims at automating the diagnosis process. Therefore, a new improved algorithm, the Growing Circle Algorithm (GCA) has been developed and successfully applied along with an automatic thresholding algorithm using bone percentage, of the image, in the extraction of the sinus areas.

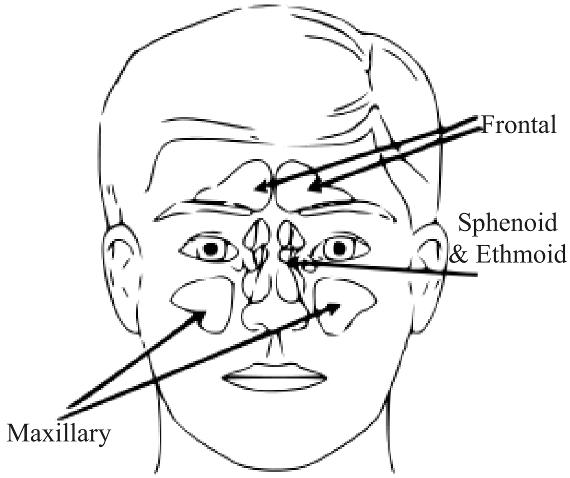

Figure 1. Normal Sinus Anatomy

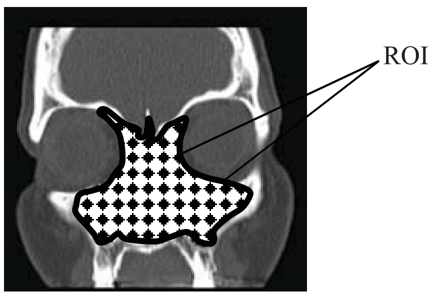

Figure 2. CT-Scans of a patient taken from frontal section.

The image analysis carried out on the CT-scans is presented in Section 2. The architecture of the proposed SDS system and the results obtained using various CT-

978-1-86135-370-2/10 ©2010 CSNDSP

scan images are presented in sections 3 and 4 respectively, whilst Section 5 concludes the work.

II. Analysis of sinus image features

The main objective of the analysis process is to find common features that can be used for identifying the ROI areas, shown in Figure 2, from the rest of a CT-image. Some features are natural in the sense that they are defined by their visual appearance in an image, while others are artificial; they result from specific manipulations of an image.

When a sinus is infected, the ROI and other parts of the human face such as the eye may appear very similar in an image. Therefore, during the ROI extraction process, textural features were ruled out due to these textural similarities.

Use of a template matching method to extract the ROI was also considered and was deemed unworkable for this application due to the variation of ROI properties such as size and shape.

Finally, the investigation led to the selection of the following attributes to extract the ROI:

- Bone Structure: As shown in Figure 2 the ROI is always surrounded by bones; in this case the bone can be used as an outline of the ROI boundary;
- Shape features: Features such as area and center of mass; and
- Referencing: Use of other objects in the CT-images such as the position of the eye as a reference for allocating the ROI position in the images.

Using the above features, an automatic sinus extraction tool was developed by combining a novel automatic segmentation method with blob analysis for extracting the ROI.

III. Methodology

CT-images of sinuses from different sections were obtained from a local hospital. As mentioned earlier this system involves two main stages (a) extraction of ROI and (b) diagnosis of the sinus area using SOM. These two stages are explained below.

A. Extraction of ROI

The sinus extraction process consists of three main stages:

- Extraction of the bone structure;
- Completing and tracing incomplete object's boundaries; and
- Identification and labeling of ROI using Blob Analysis.

1) Extraction of the bone structure

The objective of this stage is to get the outline of the bone structure surrounding the sinus areas in the CT-images. Over the last decade, several segmentation techniques were used in medical imaging applications. These include global thresholding [6,10], statistical classification [11], seeded region growing [12], region competition [13], and deformable models such as snakes [5] and balloons [14].

Extensive analysis of the sinus CT-scan images showed that the percentage of the bone structure for each section in the sinus CT images is approximately fixed with one or two percentage points difference. Hence, an algorithm was created using a threshold method based on the bone percentage of each section.

Depending on the bone percentage value, a threshold value was determined by using the cumulative histogram of each image. Figure 3 (healthy) and Figure 4 (unhealthy) show two typical CT-images and corresponding threshold values.

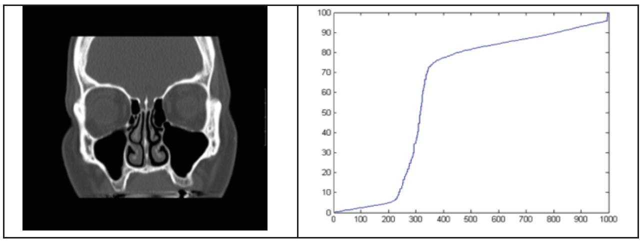

Figure 3. Cumulative histogram for healthy sinus CT-scan. Threshold value=0.4550

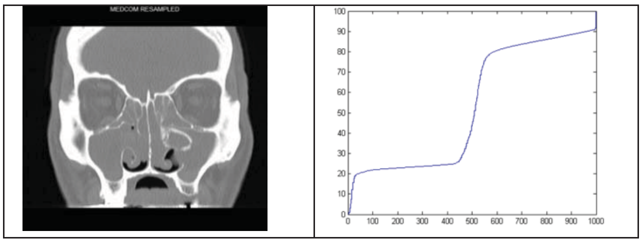

Figure 4. Cumulative histogram for unhealthy sinus CT-scan. Threshold value=0.5880

For the frontal section, the bone percentage value was approximately 20% and the corresponding segmentation results using the threshold values for two samples are shown in Figures 5 (healthy) and Figure 6 (unhealthy). This serves as the starting point for the next step in the extraction of the ROI.

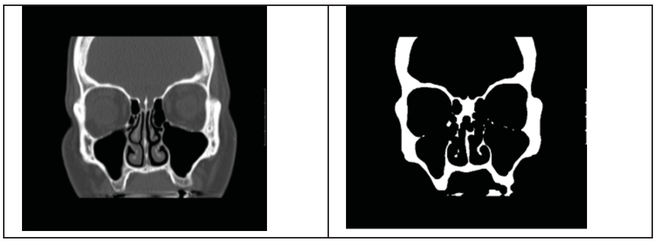

Figure 5. Output of applying threshold method to a healthy sample

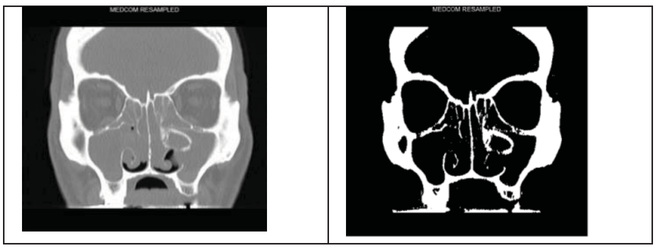

Figure 6. output of applying the threshold method to a diseased sample.

The results of applying the automatic thresholding is shown in Figure 5 and 6, the algorithm works well in extracting the bone structure in the CT-scan and in deleting the unwanted data. However, it fails in closing the boundaries that lie between the eye and the maxillary and ethmoid sinuses. This situation arises when the edge shared by two adjacent organs is weak; resulting in incomplete boundaries and therefore, two adjacent organs may be miss-detected as one object. An example is highlighted in Figure 7, where the eye and the adjacent sinus appear to have the same level of grey with an incomplete bone structure to separate. A simple threshold of the image simply shows that a separation of the two areas cannot be obtained by the sole use of the bone structure which in this case appears fragmented.

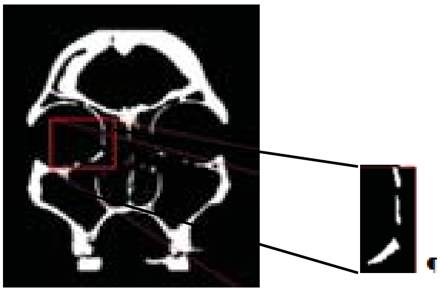

Figure 7. Fragmented edges after applying the Bone segmentation method.

2) Completing and tracing incomplete object's boundaries

The growing circle algorithm (GCA) is presented as a tool for completing fragmented boundaries in medical images and has been successfully applied to sinus images to complete the eye boundaries. This simplifies the identification process of the sinus areas and hence makes the diagnosis of sinus diseases easier.

GCA method is an iterative algorithm for closing or filling gaps in the boundaries of an object. The algorithm consists of two main steps: 1) approximation stage: to get an approximation of the shape by creating an inscribed circle within the boundaries of the object. 2) Refining stage: to refine the approximation of the shape "unpublished" [15]. Figure 8 highlights the segmented image after applying the GCA algorithm which shows that the fragmented boundary has been completely closed.

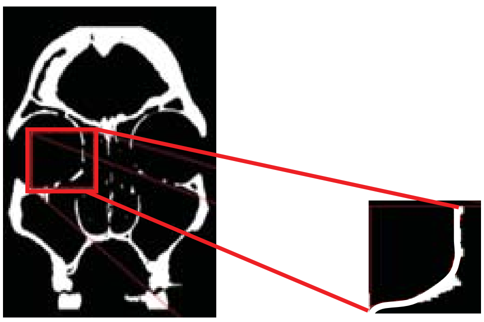

Figure 8. The segmented boundary on the left and after being completed using the GCA method on the right.

3) Identification and labelling of ROI using blob analysis

A group of pixels organized into a structure is commonly called a blob. In this phase, the objects in the binary image are labeled as different blob structures using Connected Component Analysis using four connected kernels. Blob analysis was applied to the three ROIs i.e. maxillary, ethmoide and frontal sinus areas which were labeled as blob structures, in order to get the region properties for each object. Depending on the area size and centroid features of each object, ROI areas were extracted. The results are presented in section 4.

B. Classification and Diagnosis

The second phase corresponds to the main objective of this work, i.e. to classify each ROI into three regions corresponding to air (Black), bone (White) and soft tissue (Grey). The percentage of grey region is to be used as a quantitative measure of the extent of 'disease' in the sinus area. A number of methods exist to perform such classification. Using 8-bit words to represent the level of grey, the range is from 0 (Black) to 255 (White). These are scaled down to the range of 0 to 1 for the purpose of calculating the opacity of a given ROI. Normal sinus areas tend to have an average opacity value close to zero.

A SOM with three outputs (classes) hextop topology grid was created. The SOM was provided with all of the ROI pixel values as inputs and trained to classify all the weights into 3 classes. The corresponding centroids for these classes were represented by the weights in the SOM. Once trained, the SOM was then used on the sinus area only for classifying the grey level intensity values.

Initially the SOM Neural Network was trained for 300 iterations. The resulting weights after training are shown in Table I. The classification of the SOM network has to be interpreted in terms of the physical phenomena they represent.

TABLE I. CENTROIDS OF SOM NETWORK CLASSES.

Class	Pixel intensity range
Class 1 (Air)	0.0356
Class 2 (Tissue)	0.2840
Class 3 (Bone)	0.6935

The results of the classification process are presented in the results section.

IV. RESULTS

The results of the SDS system are divided into two sections: the first for the ROI extraction and the second for the sinus diagnosis and classification.

A. ROI EXTRACTION RESULTS

A number of tests were carried out to evaluate the robustness of the system by comparing the extracted ROI images with manually extracted ROI form the sinus CT-images by an ENT consultant. Tests were performed using sinus CT-images of different sizes and disease conditions. The extraction process was very successful. The results for the sinus image are shown in Figure 9.

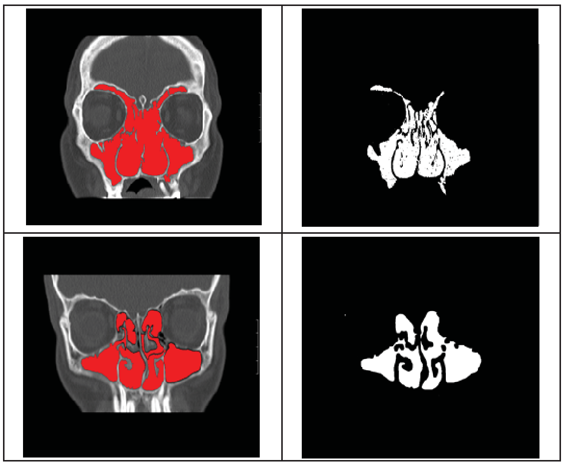

(a) (b)

Figure 9. Manually extracted ROIs (Left) and automatically extracted ROIs using the CGA algorithm.

A comparison between the manually extracted ROI and results of ROI extraction method was implemented using the sinus area feature as a measure to validate the accuracy of the algorithm. Results, shown in table II, indicate good accuracy with a maximum error of 8.8%.

TABLE II. AREA PERCENTAGE ERROR BETWEEN THE MANUALLY AND THE AUTOMATICALLY EXTRACTED AREAS.

images	Original Area	Extracted Area	Area Error Percentage%
	81729	74540	8.8%
	42701	42045	1.5%

B. *Classification and Diagnosis*

Eleven cases were analyzed and diagnosed using the proposed sinus diagnosis system. The diagnosis system gives the results as a percentage of black (how many black pixels in a given area) and percentage of grey (how many grey pixels in the area of interest).

A scale is derived from both percentages to determine whether the sinus is healthy or not; if ill how severe the infection is. The scale is defined in the following form which is used by ENT specialists:

- 0: healthy (grey %< 30%);
- 1 : First degree of infection (30% < grey% <80%); and
- 2: Severe infection (grey% > 80%).

The scale values showed in table III classify the sinus sample shown in Figure10 as healthy.

Figure 10. healthy sample of a frontal CT section.

TABLE III. DIAGNOSIS RESULTS OF A HEALTHY SINUS OF FIGURE10.

Sinus	BLACK%	GREY %	SCALE
Left ethmoid	100%	0%	0
Right ethmoid	98.2%	1.8%	0
Left maxillary	90%	10%	0
Right maxillary	95%	5%	0

Table IV presents sinus diagnosis results for the sample shown in Figure 11. The results (scale values) indicate that there is a severe infection in the left maxillary area. Otherwise, the rest of the sinus areas are healthy.

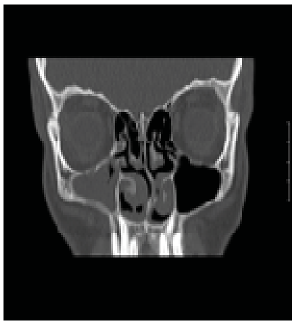

Figure 11. unhealthy sample in the right maxillary sinus area.

TABLE IV. DIAGNOSIS RESULTS OF UNHEALTHY SAMPLE **OF** FIGURE 11.

Sinus	Black%	Grey %	SCALE
Left ethmoid	85%	15%	0
Right ethmoid	82%	18%	0
Left maxillary	9%	91%	2
Right maxillary	78%	23%	0

V. CONCLUSIONS:

A new ANN-based algorithm for diagnosing sinus diseases, based on the opacity percentage scale which is normally used in the medical profession. The algorithm was extensively tested using 30 CT-images of healthy and infected sinuses with different severity of infection. The results were discussed with ENT consultant and radiologist who expressed confidence in the classification of the sinus conditions.

Future work will focus on ways of integrating the system into a CT-scanner in order to automate the sinus diagnosis process.

REFERENCES

[1] D.W. Kennedy, W.E. Bolger and S.J.Zinreich. Diseases of Sinuses Diagnosis and Management, B.C. Decker Inc. 2000.

[2] A. Natsheh, P.V.S. Ponnapalli, D. Benchebra, N. Anani, A. Al-Kholy. "Automated tool for diagnosis of sinus analysis CT-scans," Proceedings of AI 2007 the Twenty-Seventh SGAI International Conference on Innovative Techniques and Applications of Artificial Intelligence, Cambridge, UK, 2007.

[3] J. Canny. "A Computational approach to edge Detection," *IEEE Trans. Pattern Analysis and Machine Intelligence*, vol. 8, pp. 679-714,1986.

[4] X. M. Pardo, M. J. Carreira, A. Mosquera, and D. Cabello, "A snake for CT-image segmentation integrating region and edge information," Image Vis. Comput., vol. 19, pp. 461–475, 2001.

[5] M. Kass, A. Witkin, and D. Terzopoulos, "Snakes: Active contour models," Int. J. Comput. Vis., vol. 17, no. 4, 1988.

[6] P.M.Weeks, M.W. Vannier, and W.G. Stevens, "Three-dimensional imaging of the wrist," Journal of Hand- Surgery 10A (1), pp. 32–39.L.A.,1984.

[7] T. B. Sebastian, H. Tek, J. J. Crisco, and B. B. Kimia, "Segmentation of carpal bones from CT-images using skeletally coupled deformable models," Med. Image Anal., vol. 7, pp. 21–45, 2003.

[8] Grau, U. U. J. Mewes, M. Alcaniz, R. Kikinis, and S. K. Warfield, "Improved watershed transform for medical image segmentation using prior information," IEEE Trans. Med. Imag., vol. 23, no. 4, pp. 447–458,Apr. 2004.

[9] K. Haris, S. Efstratiadis, and A. Katsaggelos, "Hybrid image segmentation using watersheds and fast region merging," IEEE Trans. Image Process., vol. 7, no. 12, pp. 1684–1699, Dec. 1998.

[10] S.E. James, R. Richards and D.A.McGrouther, "Three-dimensional CT-imaging of the wrist," Journal of Hand Surgery 17B (5), pp. 504–506,1992.

[11] R.O.Duda, P.E.Hart, Pattern classification and scene analysis. John Wiley & Sons.1973.

[12] R.Adams, L.Bischof, "Seeded region growing," IEEE Trans Pattern Analysis and Machine Intelligence 16, vol. 6, pp. 641–647, 1994.

[13] S.C. Zhu, A.L.Yuille, "Region competition: unifying snakes, region growing, and Bayes/MDL for multiband image segmentation," IEEE Trans. Pattern Analysis and Machine Intelligence 18, vol. 9, pp. 884– 900, 1996.

[14] L.D.Cohen, I.Cohen, "Finite element methods for active contour models and balloons for 2D and 3D images," IEEE Trans. Pattern Analysis and Machine Intelligence 15, vol. 11, pp. 1131–1147,1993.

[15] D. Benchebra, P. Ponnapalli, N. A. Anani and A. R. Natsheh, "A novel algorithm for completing fragmented boundaries in images," submitted to the 7th IEEE, IET International symp. on comm. sys, networks and digital signal processing (CSNDSP 2010), Newcastle Upon Tyne, UK, 21-23 July 2010, unpublished.